## ARTICLES

# Semiclassical description of cyclotron resonance in quasi-two-dimensional organic conductors: Theory and experiment

Stephen Hill
*National High Magnetic Field Laboratory, 1800 East Paul Dirac Drive, Tallahassee, Florida 32310*
(Received 30 September 1996)

We discuss cyclotron-resonance-like behavior in quasi-two-dimensional organic conductors, both from a theoretical perspective and from an experimental point of view. We demonstrate how the conductivity in the least dispersive direction can dominate the magnetoelectrodynamic response of highly anisotropic metals. Consequently, we develop a detailed semiclassical model for the conductivity in this direction, taking into consideration the unique Fermi surface topologies common to these materials. This can result in multiple cyclotron-resonance-like features in the conductivity along the least conducting direction, which arise from periodic motion in a plane perpendicular to the applied magnetic field; we refer to these features as ''periodic orbit resonances.'' It is shown that the details of these periodic orbit resonances are highly sensitive to the precise shape of the Fermi surface; indeed, both quasi-two-dimensional, and quasi-one-dimensional, Fermi surface sections will contribute to this effect. We also discuss compelling experimental evidence supporting our model, as well as several other consequences of such a semiclassical treatment; e.g., magnetoresistance and periodic orbit resonance linewidths. The outcome of this work is a clearer understanding of cyclotron-resonance-like features observed recently in several bis(ethylenedithio)-tetrathiafulvalene charge-transfer salts. In light of our findings, we urge caution when analyzing experimental data. In particular, care should be exercised in experiments on materials possessing both quasi-one- and two-dimensional Fermi surfaces, bearing in mind that either type of carrier can contribute to the periodic orbit resonances. [S0163-1829(97)02708-2]

## I. INTRODUCTION

Organic conductors have, in recent years, attracted considerable interest, largely because of the rich variety of exotic properties they exhibit;[1–4] e.g., superconductivity, antiferromagnetism. Many of these properties challenge our current theoretical understanding of solid state physics. A particular attraction to the experimentalist is the possibility, through subtle chemistry, to alter the structures of these materials and therefore investigate the correlation between structure and properties.[1–4] As a result, there has been a strong bias towards ''fermiology'' studies, using high magnetic fields,[4] e.g., measurements of the Shubnikov–de Haas (SdH) and de Haas–van Alphen (dHvA) effects, from which information about Fermi surfaces may be obtained.[5]

In this respect, organic conductors belonging to the $(BEDT\text{-}TTF)_2X$ family [where BEDT-TTF denotes bis(ethylenedithio)-tetrathiafulvalene] are ideal: they possess relatively simple quasi-two-dimensional (Q2D) and quasi-one-dimensional (Q1D) Fermi surfaces,[2] the quality of these materials is usually extremely high; and they exhibit extremely rich pressure, temperature, magnetic field, phase diagrams.[1–4] Extensive thermodynamic and transport measurements in high magnetic fields have been performed in order to characterize the electronic structures of these materials through quantum oscillations in e.g., the magnetoresistance (SdH effect) or, the magnetization (dHvA effect).[3,4] Furthermore, although at first sight fairly simple, the Fermi surface topologies of organic conductors are quite unique, due to the inherent ''three dimensionality'' of their structures;[3] this leads to interesting angle-dependent effects, e.g., angle-dependent magnetoresistance oscillations (AMRO).[3–15]

A precise theoretical understanding of the ''fermiology'' of organic conductors is essential in view of the wider interests these materials attract, particularly since such studies provide important band-structure parameters that may have implications for theories of, e.g., superconductivity.[2,16] As recent studies on BEDT-TTF salts have shown, the theoretical framework describing the SdH and dHvA effects becomes unreliable at high magnetic fields.[17,18]

While the magneto-transport properties have been extensively studied, relatively few magneto-optical investigations have been reported.[19–27] Although optical data for conducting systems can be complicated to interpret (relying on a good knowledge of several key parameters such as the absolute conductivity of the material, scattering times, and any anisotropy in these numbers), the potential rewards from such measurements are tremendous,[27,28] as we shall demonstrate in this paper.

Besides experiment, many theoretical papers have also focused on the dc transport properties of organic conductors.[7,9,11,13–15,29] However, there are few cases where the precise Fermi surface topology is taken into consideration to explain the optical, or finite frequency, response.[22,24,26,30] This is surprising, since a semiclassical treatment, which has been extremely successful in describing AMRO,[7,9,11,13–15] is no more complicated for the ac case. We

 

will show that the consequences of such a treatment for the Q2D BEDT-TTF salts result in some striking predictions concerning the measurement of cyclotron resonance (CR); furthermore, when we consider these predictions in the context of a real experimental situation, it becomes clear that interpretation of CR data is by no means straightforward. All of the properties discussed in this paper will stem from the unique Fermi surface topologies common to these materials, where dispersion in the least conducting direction turns out to be of utmost importance. We will also show how several other properties, which are unique to this class of conductor, contribute to a novel CR behavior.

We wish to stress from the outset that our approach is different from that adopted by Gor'kov and Lebed',[30] who also predict a novel CR behavior in Q1D organic conductors. Although their approach is totally justified, we will show that the experimental conditions necessary for the observation of Q1D CR, as predicted by Gor'kov and Lebed', are unlikely to be realized in the materials that we focus on in this paper.

This paper is organized as follows. In Sec. II, we discuss the motivation for the present study. In Sec. III we develop a theoretical model for the conductivity of a Q2D system along its least conducting direction; in the same section, we go on to examine the implications of this model for CR and magnetoresistance, as well as discussing Q1D CR and resonance linewidths. In Sec. IV, we consider a real experimental situation, illustrating the overwhelming contribution from the conductivity in the least dispersive direction, to the very-far-infrared response of such a sample. Finally, in Sec. V, we present conclusions and a summary.

## II. CASE FOR THE PRESENT STUDY

Just as in the case of dc measurements, correct interpretation of CR is obviously of immense importance, since effective mass values and information about scattering mechanisms are readily available by this technique. This is particularly so in the Q2D BEDT-TTF salts, where recent CR measurements indicate effective masses that are substantially lower than those deduced from dc transport measurements.[19–22,25,26] This has led several workers to suggest that strong electron-electron interactions result in a renormalization of the thermodynamic density of states at the Fermi level, thereby yielding an energy- or wave vector-dependent effective mass.[19–22,24–26]

The first report of CR in the BEDT-TTF family was by Singleton *et al.*,[19] who observed two CRs in the $\alpha$-(BEDT-TTF)$_2$KHg(NCS)$_4$ salt. These early findings were controversial for a number of reasons, not least because of the lower than expected CR mass. Since then, considerable advances in experimental technique have been made, and several groups have reported findings similar to those in the earlier report by Singleton and co-workers.[21,22,24–26] However, even assuming a frequency-dependent effective mass, much of the data remains difficult to interpret in terms of a simple CR picture. This is best illustrated by considering data obtained for the salt, $\alpha$-(BEDT-TTF)$_2$NH$_4$Hg(NCS)$_4$, for which several CR studies have been reported.[20–22,24–26]

$\alpha$-(BEDT-TTF)$_2$NH$_4$Hg(NCS)$_4$ is a Q2D metal with a Fermi surface comprising a single closed Q2D cylinder and a pair of Q1D open sheets [see Fig. 1(a)].[31,32] For such a Fermi surface, one usually expects no CR from the open sheets and only a single CR from the closed cylinder at a frequency $\omega_c = e\mathbf{B}/m^{2D}$, where $m^{2D}$ is the effective mass of the Q2D carriers averaged over the cylinder. However, several recent studies have resolved multiple (up to three) resonances for this material.[21,22,26] Attempts to account for these results in terms of Azbel'-Kaner-type resonances,[33] and/or Gorkov' and Lebed's Q1D resonances,[30] are most probably incorrect, for reasons that will be discussed in Sec. IV, where we will discuss existing magneto-optical data.

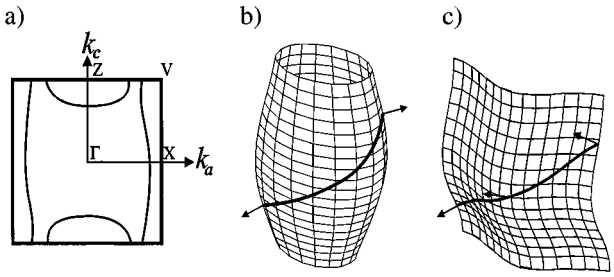


FIG. 1. (a) The two-dimensional Fermi surface of $\alpha$-(BEDT-TTF)$_2$NH$_4$Hg(NCS)$_4$ (Ref. 32) and three-dimensional representations of (b) a warped Q2D Fermi cylinder, and (c) a warped Q1D Fermi sheet; the warping in (b) and (c) has been exaggerated for the sake of clarity. The thick lines in (b) and (c) represent quasiparticle trajectories around and/or across these Fermi surfaces, caused by the application of a magnetic field (the trajectories are constrained to planes perpendicular to this field); arrows normal to the Fermi surfaces demonstrate how the velocities of carriers will change as they sweep around/across these Fermi surfaces.

A breakthrough in the understanding of the very-far-infrared response of the Q2D BEDT-TTF salts has come about via the use of resonant cavity structures.[22,24,26–28] This has permitted extremely sensitive measurements on single crystals, in a controlled environment, where the polarizations of the ac electric and magnetic fields are well known. In such experiments, it is consistently found that measurements of the interplane conductivity (least conducting direction which we shall refer to as the $z$ direction from here on) yield the best results.[24,26,34] The recent observation of quantum oscillations in the $z$-axis conductivity $[\sigma_{zz}(\omega)]$ is a clear indication that these materials really behave like three-dimensional metals,[24,26,34] albeit highly anisotropic ones. Even more remarkable is the failure to observe quantum oscillations from measurements of the in-plane conductivity $[\sigma_{||}(\omega)]$.[24]

We save an in-depth discussion of in-plane versus interplane measurements of $\sigma(\omega)$ until Sec. IV. Instead we will focus on the $z$-axis response, which, from the above experimental considerations, appears to be the most illuminating direction.

## III. THEORY

The basis for the predictions of this paper relies on the fact that we may treat the very-far-infrared (microwave) response of these materials semiclassically; we do so by computing the conductivity through the Boltzmann transport equation.[35] As mentioned above, several aspects of the dc transport have been explained successfully by this method. A

typical approach involves modeling the Fermi surface, then calculating the group velocity of carriers on the Fermi surface, and finally computing the velocity-velocity correlation function; arriving at an expression for the conductivity is then straightforward.

We will start by considering a typical BEDT-TTF salt, subjected to a magnetic field. The field causes carriers to follow periodic $k$-space orbits about either closed or open Fermi surfaces, and can result in complex real-space trajectories; this is due to the weakly warped nature of these Fermi surfaces along their least dispersive directions, as illustrated in Fig. 1. Such complex real-space trajectories lead to resonances in the velocity-velocity correlation function when the magnetic field points along certain ''magic'' angles; this is the physical basis for AMRO. For the purposes of this paper, we shall concentrate on resonances of the high-frequency conductivity, which occur at ''magic'' frequencies, as opposed to ''magic'' angles. These resonances, which we shall refer to as ''periodic orbit resonances'' (PORs), are closely related to CR and arise from the periodic $k$-space motion.

### A. Model for a Q2D Fermi surface cylinder

As a model Q2D Fermi surface, we will consider a weakly warped cylinder with an elliptical cross section [Fig. 1(b)]; the cylinder is elongated along the $z$ axis (least conducting axis). The precise nature of this warping depends intimately on the mechanism by which carriers can ''hop'' between adjacent conducting layers of BEDT-TTF molecules.[36] Early attempts to model AMRO data assumed the simplest possible form for this ''hopping,'' namely, in terms of a small, but finite, interlayer transfer integral $\xi_\perp$ ($\ll\varepsilon_f$).[7,9] More sophisticated calculations take into account an additional in-plane ''hopping'' component, such that the warping direction tilts away from the cylinder axis by some arbitrary angle $\theta$.[10]

In an attempt to account for what we now understand to be Q1D AMRO, in the $\alpha$-phase BEDT-TTF salts,[13,15] Yagi and Iye[14] have considered more complex forms for the interlayer transfer integral, whereby $\xi_\perp$ depends on the in-plane wave vectors $k_x$ and $k_y$; their calculations demonstrate that AMRO are rather sensitive to the explicit dependence of $\xi_\perp$ on $k_x$ and $k_y$.

Following the approach of Yagi and Iye,[14] we will also assume that $\xi_\perp$ depends on $k_x$ and $k_y$. We choose a $(d_{xx}+d_{yy})$-type warping symmetry, and a simple example for the energy dispersion relation in this case is given by

$$E=\left(\frac{\hbar^2k_x^2}{2m_{xx}}+\frac{\hbar^2k_y^2}{2m_{yy}}\right)-2\xi\cos(k_z\mathbf{c})\frac{k_x^2+k_y^2}{\overline{k_{f\|}^2}}, \tag{1}$$

where $4\xi$ ($\ll\varepsilon_f$) defines the $z$-axis bandwidth, $\overline{k_{f\|}}$ is the average in-plane Fermi wave vector, $m_{xx}$ and $m_{yy}$ are in-plane components of the effective mass tensor, and $\mathbf{c}$ is the interlayer spacing. Yagi and Iye have shown that $d_{xx}$-type warping produces AMRO that are almost identical to the AMRO for $s$-type ($k_x,k_y$–independent) warping, when the field is rotated in the $(k_x,k_z)$ plane.[14] Therefore, $(d_{xx}+d_{yy})$-type warping will produce an AMRO effect, analogous to the $s$-type case, for rotation in any plane, albeit an anisotropic AMRO effect; such behavior is, indeed, found experimentally.[10,11] As a special case, we note that for a Fermi cylinder with a circular cross section, the $(d_{xx}+d_{yy})$ symmetry reduces to $s$-type symmetry.

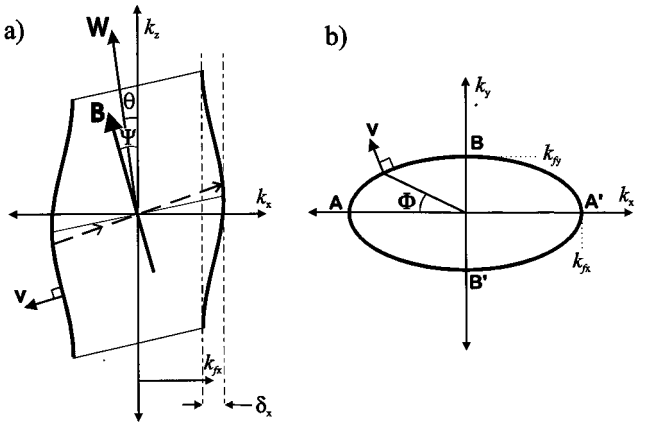


FIG. 2. Cross sections of the Fermi surface described by Eq. (2) (a) in the $(k_x,k_z)$ plane, and (b) in the $(k_x,k_y)$ plane; in (a) the warping has been exaggerated for the sake of clarity. The Greek and italicized symbols are explained in the text. The purpose of the labels $A$, $A'$, $B$, $B'$ is to aid discussion (see text). The vector **W** points along the warping axis, which is tilted away from the $k_z$ axis by the small angle $\theta$. The applied magnetic field points along **B** and may be tilted away from the $k_z$ axis by a small angle $\Psi$; the dashed line, perpendicular to the field direction, indicates the path of a carrier around the Fermi surface. The arrows labeled **v**, in (a) and (b), which are perpendicular to the Fermi surface, represent the velocity of a carrier at the Fermi surface.

For a more general treatment, we take into consideration a slight tilting of the warping axis away from the $z$ axis (cylinder axis). In order to calculate the velocities of carriers at the Fermi surface, we write down a representation of the Fermi surface in terms of the cylindrical coordinates $k_z$ and $\Phi$:

$$\begin{aligned} k_x&=k_{fx}[1+\delta_x\cos\{(k_z-\kappa\cos\Phi)\mathbf{c}\}]\cos\Phi,\\ k_y&=k_{fy}[1+\delta_y\cos\{(k_z-\kappa\cos\Phi)\mathbf{c}\}]\sin\Phi. \end{aligned} \tag{2}$$

In the above expression, $k_{fx}$ and $k_{fy}$ are the Fermi wave vectors along the $k_x$ and $k_y$ axes, $\delta_x$ and $\delta_y$ are the amplitudes of the warping in the $k_x$ and $k_y$ directions, and $\kappa$ is related to the tilting angle $\theta$ such that $\kappa=k_{fx}\tan\theta$. Equation (2) assumes that the in-plane component of the warping is directed along $k_x$. We shall additionally assume, in our subsequent analysis, that the angle $\theta$ is small. Figure 2 shows two cross-sectional representations of the Fermi surface described by Eq. (2) [see also Fig. 1(b)].

In order to calculate the longitudinal conductivity $\sigma_{zz}$, we need to know the $z$ components of the carrier velocities $\mathbf{v}_z$ at the Fermi surface. This is done simply by calculating the $z$-axis dispersion, i.e.,

$$E_z=\varepsilon_f-\left(\frac{\hbar^2k_x^2}{2m_{xx}}+\frac{\hbar^2k_y^2}{2m_{yy}}\right), \tag{3}$$

substituting for $k_x$ and $k_y$ from Eq. (2), and then, by taking the derivative $\partial E_z/\partial k_z$. In doing so, we obtain the following expression:

$$\frac{\hbar}{\varepsilon_f \delta_x \mathbf{c}} \mathbf{v}_z = \sin(k_z \mathbf{c})[(1+\Delta)+(1-\Delta)\cos 2\Phi] - \left(\frac{\kappa \mathbf{c}}{2}\right)\cos(k_z \mathbf{c})[(3+\Delta)\cos\Phi + (1-\Delta)\cos 3\Phi], \tag{4}$$

where $\Delta = \delta_y/\delta_x$. In order to arrive at Eq. (4), we have neglected terms of order $\delta_x^2$ and $\delta_y^2$, we have assumed that the product $\kappa \mathbf{c} \ll 1$ (i.e., the angle $\theta$ is small), and we have used trigonometric relationships to simplify the final expression.

We now consider the effects of applying a dc magnetic field along the $z$ direction. This causes carriers to circulate, in a plane perpendicular to the applied magnetic field ($k_x, k_y$ plane, in this case), with a characteristic cyclotron frequency, $\omega_c = eB/m_\parallel$; $B$ is the applied field strength and $m_\parallel$ is the average in-plane effective mass. We can take this into consideration in Eq. (4), by setting $\Phi = (\omega_c t + \phi)$, where $\phi$ is now the azimuthal coordinate for a particular carrier at time $t=0$. In fact, it turns out that the role of the parameter $\kappa$ in Eqs. (2) and (4) may equally represent a tilting of the applied magnetic field away from the $z$ direction; this is also depicted in Fig. 2, where the field is tilted away from the $z$ axis, along $k_x$, by a small angle $\Psi$. Due to approximations made in the derivation, Eq. (4) is only valid provided that the angle $(\theta - \Psi)$ is small. In the case of a tilted field, the following modifications should also be made to Eq. (4): $m_\parallel \rightarrow (m_\parallel/\cos\Psi)$ and $\kappa = k_{fx}\tan(\theta - \Psi)$.

*Now we can see the remarkable properties of the z-axis velocity*, namely, that if we apply a magnetic field in the $z$ direction, the $z$-axis velocity changes with time.[37] *In fact*, it contains oscillatory components, not only at a frequency $\omega_c$ but also at $2\omega_c$ and $3\omega_c$. Furthermore, if the field is applied parallel to the warping axis (i.e., if $\theta = \Psi$) and provided $\delta_x \neq \delta_y$, the only oscillatory component has a characteristic frequency of $2\omega_c$, rather than $\omega_c$. Even in the case where $\delta_x = \delta_y$, $\mathbf{v}_z$ will still oscillate at a frequency of $\omega_c$ provided that the warping direction is not coincident with the $z$ axis; if these directions do coincide, then $\mathbf{v}_z$ contains no oscillatory components. The physical origin of this effect is the periodic motion of carriers about the Fermi surface, coupled with the $k_x, k_y$ dependence of the $z$-axis dispersion.

To see what effect this has on the frequency-dependent conductivity $[\sigma_{zz}(\omega)]$ we appeal to the Boltzmann transport equation,[35]

$$\sigma_{zz}(\omega) = \frac{2e^2}{V}\int d^3k\left[-\frac{df(k)}{dE(k)}\right]\mathbf{v}_z(k,\ t=0) \times \int_{-\infty}^{0}\mathbf{v}_z(k,t)\exp\{[(1/\tau)-i\omega]t\}dt, \tag{5}$$

where the first integral is a summation over all $k$ states, while the remainder of the expression is the so-called velocity-velocity correlation function, representing the correlation between the velocity of a carrier at a general time $t$, with its velocity at $t=0$; $df(k)/dE(k)$ is the derivative of the Fermi function and $\tau$ is the scattering time. We substitute for the $z$-axis velocity from Eq. (4) and, since we are interested in dealing only in the low-temperature limit of $\sigma_{zz}(\omega)$, we can greatly simplify the problem by considering only states at the Fermi surface since $df(k)/dE(k)$ will be zero elsewhere. Due to the symmetry of the Fermi surface, we integrate over the cylindrical coordinates $k_z$ and $\phi$. The velocity-velocity correlation function results in resonances in $\sigma_{zz}(\omega)$ at frequencies $\omega_c$, $2\omega_c$, and $3\omega_c$ as can be seen from the following final expression:

$$\sigma_{zz} = \text{const}\times\left[\frac{1}{16}\{2(1+\Delta^2)(3+\Lambda^2)+(1-\Delta^2)(1-\Lambda^2)\}\Omega_0 + \frac{1}{16}(1-\Delta)^2\{(3+\Lambda^2)+(1-\Lambda^2)\}\Omega_1 + \left(\frac{\kappa \mathbf{c}}{8}\right)^2\{(3+\Lambda^2)(3+\Delta)^2+2(1-\Lambda^2)(3+\Delta)\}\Omega_2 + \frac{1}{2}\left(\frac{\kappa \mathbf{c}}{8}\right)^2(1-\Delta) \times\{2(3+\Lambda^2)(1-\Delta)+(1-\Lambda^2)(3+\Delta)\}\Omega_3\right], \tag{6}$$

where $\Lambda$ is the ellipticity of the Fermi surface, given by the ratio $k_{fy}/k_{fx}$, and

$$\Omega_n = \left[\frac{1+i(\omega - n\omega_c)\tau}{1+(\omega-n\omega_c)^2\tau^2}\right]+\left[\frac{1+i(\omega+n\omega_c)\tau}{1+(\omega+n\omega_c)^2\tau^2}\right]. \tag{7}$$

Figure 3(a) shows a simulation of the real part of $\sigma_{zz}(\omega)$, plotted as a function of magnetic field (normalized to $m_\parallel \omega/e$), for several values of the angle $(\theta - \Psi)$. According to Eqs. (1) and (2), and for the purposes of the simulations, we have assumed that $\Delta = \Lambda^2$. Furthermore, in order to generate meaningful results, we have chosen input parameters that correspond to a real system, namely the Q2D Fermi surface of $(BEDT\text{-}TTF)_2NH_4Hg(NCS)_4$. These parameters are: an ellipticity of $\Lambda = 0.65$, and values for the Fermi wave vectors of $k_{fx} \approx (\pi/\mathbf{c})$ and $k_{fy} \approx (2\pi/3\mathbf{c})$;[11,32] we also chose a value of $\omega\tau = 15$ for the data in Fig. 3(a).

As predicted, three resonances in $\sigma_{zz}(\omega)$ can be seen in Fig. 3(a), one at the fundamental ''periodic orbit resonance'' (POR) position, together with second and third harmonics. It is apparent from Fig. 3(a) that, up to at least 5°, the POR behavior is dominated almost entirely by the second harmonic. As the field is tilted away from the warping direction, the fundamental resonance gains strength and a third harmonic becomes apparent on the low-field side of the strong second harmonic.

Figure 3(b) shows further simulations of the real part of $\sigma_{zz}(\omega)$, this time, for different ellipticities $\Lambda$; the warping axis is tilted 5° away from the $z$ axis and the field is applied parallel to the $z$ axis for the purpose of these simulations, i.e., $\theta = 5°$ and $\Psi = 0°$. Figure 3(b) demonstrates that, even for ellipticities close to unity, a strong second harmonic contribution to the POR is still expected.

We contrast POR behavior with CR, since the latter is a direct consequence of the cyclotron motion, both in real space and in $k$ space, while the former is an indirect consequence of the cyclotron motion in $k$ space resulting in periodic motion in real space. In this respect, the origins of the first and second POR harmonics are quite different. The second harmonic results from the $(d_{xx}+d_{yy})$ symmetry consid-

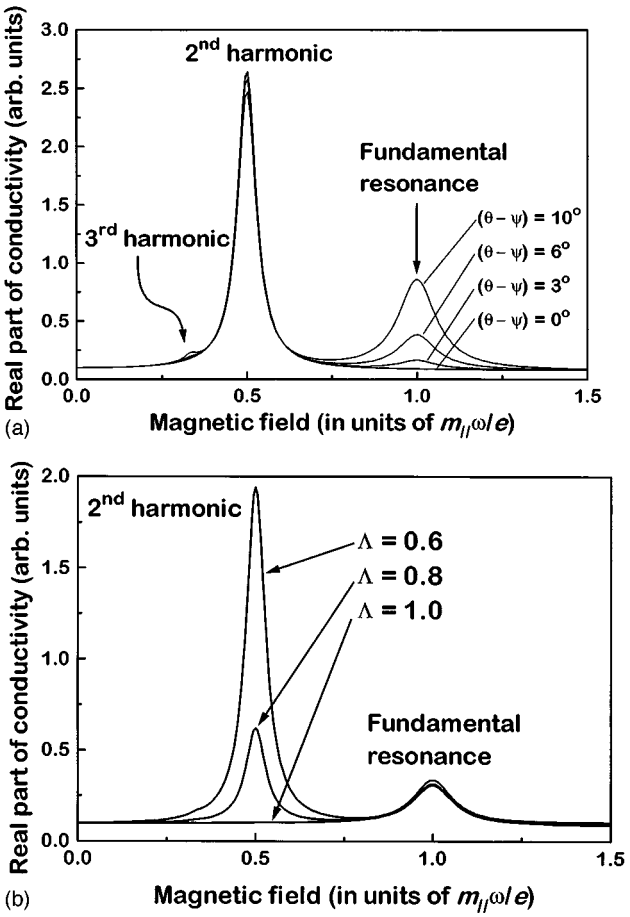


FIG. 3. Simulations of the real part of $\sigma_{zz}(\omega)$ plotted against magnetic field (normalized to $m_{\|}\omega/e$), as a function of (a) the angle $(\theta-\Psi)$, assuming $\Lambda=0.65$, and (b) the ellipticity, $\Lambda$, assuming $\theta=5°$. Up to three resonances can be seen at positions corresponding to the fundamental, second and third harmonics.

ered for the $z$-axis dispersion; due to the symmetry between points at $\pm k$ (e.g., points $A$ and $A'$, or $B$ and $B'$, in Fig. 2), the $z$-axis velocity undergoes two cycles during one cyclotron period. Meanwhile, the fundamental POR occurs because of a tilting of the warping axis ($\theta\neq\Psi$), and is very similar in origin to the AMRO effect. Therefore, one might expect the intensity of the fundamental POR to show oscillations similar to the AMRO, whereas the second harmonic should be relatively insensitive to rotation (at least for small angles).[38] The third harmonic is an interference between the fundamental and second harmonics.

Up to this point, we have considered a relatively simple 2D cross section for the Fermi surface, yet we see up to three POR harmonics. If we consider a more general shape for the Q2D Fermi surface, including deviations from a perfect ellipse, then Eq. (2) should be rewritten as a Fourier series in powers of $\cos\Phi$ and $\sin\Phi$. This will lead to higher and higher order POR harmonics; in particular, one might expect to see a second harmonic of the second harmonic, i.e., a fourth harmonic.

Our model has demonstrated that PORs are a general feature in the high-frequency $z$-axis conductivity for Q2D BEDT-TTF salts. This behavior arises because of the finite dispersion in the least conducting direction. The details of the resulting PORs are found to be extremely sensitive to the way in which an idealized two-dimensional Fermi cylinder is deformed, both along its axis, and through its cross section. As we shall discuss in the following sections, PORs are not limited to Q2D Fermi surfaces, i.e., cyclotron motion is not a prerequisite.

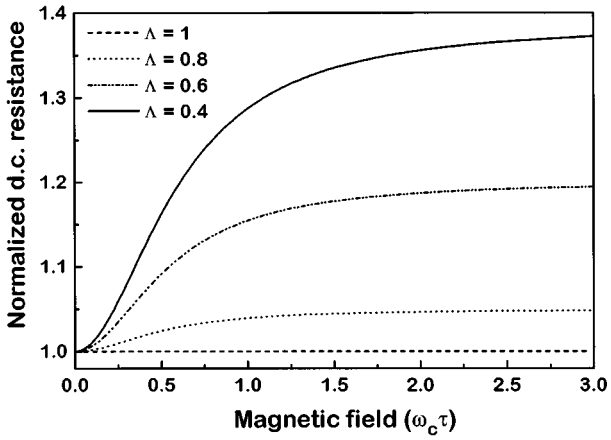


FIG. 4. A simulation of the dc $z$-axis resistance $\rho_{zz}$ (normalized), plotted against $\omega_c\tau$ ($\propto B$), for several different ellipticities; $\theta=\Psi=0°$.

### B. Longitudinal dc magnetoresistance

An interesting aside is to consider the effect of $(d_{xx}+d_{yy})$-type warping on the longitudinal dc magnetoresistance ($\rho_{zz}=1/\sigma_{zz}$) of the BEDT-TTF salts; by $\rho_{zz}$, we imply the $z$-axis (interplane) resistance, with the magnetic field also applied along this direction. For a long time, it has been a puzzle why $\rho_{zz}$ always exhibits a considerable magnetoresistance effect, as well as SdH oscillations at high fields.[39]

Figure 4 shows a simulation of the normalized dc magnetoresistance for several different ellipticities $\Lambda$, plotted as a function of $\omega_c\tau$ ($\propto B$); for the purposes of these simulations, $\theta$ and $\Psi$ are taken to be zero. It can be seen from Fig. 4, that an elliptical Fermi surface produces a significant magnetoresistance effect. Magnetoresistance is also predicted for the case of a Fermi surface having circular cross section, provided $\Delta\neq1$, i.e., $\delta_x\neq\delta_y$. However, the most remarkable result for $\Delta\neq1$, is that magnetoresistance is predicted no matter what direction the magnetic field is applied.

Any modulation of the $z$-axis velocity will lead to magnetoresistance in this direction. The reason this occurs for our model Fermi surface (see Fig. 2) when $\Lambda\neq1$, is because the $z$-axis velocity is different[37] at points $A$ and $A'$ than at points $B$ and $B'$ [see Fig. 2(b)], even for the case where $\theta=\Psi=0$. For $s$-type warping symmetry, no magnetoresistance is predicted when the magnetic field direction is coincident with the axis of warping, e.g., when $\theta=\Psi$; this is because the $z$-axis velocity is unchanged by applying a magnetic field, i.e., the $z$-axis dispersion is the same at points $A$, $A'$, $B$, and $B'$ [see Fig. 2(b)]. This feature of the magnetoresistance is the most compelling evidence supporting our choice of a lower symmetry of warping.

### C. Q1D periodic orbit resonances

Having worked through the case for a Q2D Fermi cylinder, we now consider the role of Q1D carriers (common to

most BEDT-TTF salts) in the $z$-axis response. Clearly, any periodic modulation of the $z$ component of the group velocities of carriers on such a Fermi surface will lead to PORs in $\sigma_{zz}(\omega)$. It is quite easy to envisage such a modulation from inspection of Fig. 1. However, choosing an appropriate functional form for the warping of a Q1D Fermi surface sheet is not quite so straightforward, and is beyond the scope of this paper.[15] Nevertheless, if the $z$-axis bandwidths are comparable for the Q1D and Q2D Fermi surfaces, then both types of carrier should produce similar POR effects,[40] distinguishable only by their fundamental ''cyclotron'' frequencies. The term ''cyclotron'' frequency is used loosely here to represent the frequency with which carriers return to the same point in the $(k_x,k_y)$-plane; in the Q2D case this occurs because the carriers execute closed orbits, whereas, in the Q1D case, carriers continually sweep across the $(k_x,k_y)$-plane, periodically Bragg scattering back to the same point. The frequency with which Q1D carriers traverse the $(k_x,k_y)$-plane say, from $+k_{fx}$ to $-k_{fx}$, is given by[2]

$$\omega_c^{\mathrm{Q1D}}=\frac{eB}{m_{\mathrm{Q1D}}}\,k_{fy}^{\mathrm{Q1D}}\mathbf{b}, \tag{8}$$

where $m_{\mathrm{Q1D}}$ is the average effective mass of carriers on a Q1D Fermi surface defined by $k_y\approx\pm k_{fy}^{\mathrm{Q1D}}$, and $\mathbf{b}$ is the lattice constant in the $y$-direction. Therefore, for a system with both Q1D and Q2D Fermi surfaces, a separate sequence of Q1D POR harmonics may be expected in the $z$-axis conductivity, in addition to the Q2D POR.

This type of resonant effect should not be restricted to the BEDT-TTF salts; indeed, it should be a general feature of highly anisotropic conducting systems. In Sec. IV, we will discuss some of the experimental criteria for observing POR features in the conductivity along the least dispersive directions in low dimensional conductors. However, the point we wish to emphasize here, is that it is along the least conducting directions that we expect to observe these effects; this contrasts the Gor'kov and Lebed' resonances,[30] which are predicted for measurements along the high conductivity axis of Q1D organic conductors such as $TMTSF_2X$ (where $X=PF_6$, $ClO_4$, $AF_6$, and TMTSF denotes tetramethyltetraselenafulvalene).[2]

We have demonstrated that interpretation of $\sigma_{zz}(\omega,B)$ is by no means straightforward. In particular, PORs are expected from both Q2D and Q1D Fermi surfaces. Furthermore, these PORs will come in sequences of harmonics, periodic in $1/B$, where the periodicity is related to the effective masses of either the Q2D or Q1D carriers. Due to the similarity between PORs and AMRO it should be possible to distinguish between the Q2D and Q1D POR contributions from their angle dependence. From the relative strengths of the POR subharmonics, one could, in principle, obtain information about the precise deformations of the Q2D and Q1D Fermi surfaces. This offers an exciting method for determining the fermiology of low-dimensional conductors.

### D. Discussion of resonance linewidths

We end this section by discussing the linewidths and temperature dependence of the POR behavior described above. There is often confusion regarding the mechanisms that lead to a broadening of cyclotronlike resonances, of which the PORs are a subset. The resonance linewidth is governed by the scattering time $\tau$ in Eq. (7). This scattering time may contain many different contributions from, e.g., impurities, boundaries, electron-phonon scattering, electron-electron scattering, etc.[35] However, this scattering time is not necessarily the same as the one which is deduced from SdH or dHvA experiments.[35,5] Furthermore, the temperature dependence of CR/POR is expected to be completely different from the temperature dependences of the SdH and dHvA effects.

The criteria for the observation of quantum oscillatory effects (i.e., SdH and dHvA) are far more stringent, being governed by so-called ''phase smearing'' factors;[5] this ''phase'' is completely different from the phase $\Phi$ appearing in Eq. (2), and is related to the area enclosed by a closed orbit in $k$ space. In this regard, it is not only the scattering time $\tau$, which is important, but also any other processes that lead to a distribution of this phase, when averaged over all carriers in the crystal. The main phase smearing contributions come from the effects of finite temperature, scattering, and sample inhomogeneities.[5] As a result of this, quantum oscillations are generally not observed in BEDT-TTF salts for temperatures above 4.2 K and magnetic fields below 5 T.[3] Meanwhile, most of the available magneto-optical data clearly show CR-like features at fields well below 5 T.[21–26] Furthermore, some groups claim to observed CR features in BEDT-TTF salts at temperatures above 20 K.[25] A finite temperature merely redistributes carriers among states close to the Fermi energy, thus, for a parabolic band, the ''cyclotron'' motion remains unaffected. The only way the temperature can have an effect on this motion is indirectly, through the temperature dependence of scattering mechanisms such as electron-phonon, or electron-electron.

Aside from the temperature dependence, the scattering times deduced from SdH and dHvA measurements can be misleading, since they do not necessarily reflect the true scattering time. This is because the effects of sample inhomogeneities[41] on SdH, or dHvA oscillation amplitudes are indistinguishable from the effects of real scattering processes.[5] Typical scattering times deduced from available magneto-optical data indicate values of $\omega\tau$ in excess of 15 (at 50 GHz), i.e., $\tau\approx 4\times10^{-11}$ s;[22] this compares to a value of about $2\times10^{-12}$ s deduced from dHvA measurements.[3] To place this in perspective, we note that a scattering time, $\tau=4\times10^{-11}$ s, is still an order of magnitude shorter than the scattering times found for the highest quality artificial semiconductor devices.[22] We also note that a similar scattering time of $\tau=5\times10^{-11}$ s, has recently been reported from CR measurements on another organic conductor, $(DMe\text{-}DCNQI)_2Cu$.[27]

The factor of 10, or so, difference between the scattering times deduced from magneto-optical studies, and from SdH or dHvA measurements, raises some important issues. In particular, it suggests that the dominant SdH/dHvA ''phase smearing'' occurs as a result of sample inhomogeneities (over a macroscopic length scale),[41] rather than impurity scattering. Inhomogeneities may occur during the growth process. Crystal growth typically takes place over several weeks, and as the samples grow in size, the growth conditions change. Recent attempts have been made to monitor

TABLE I. A list of key parameters that govern the electrodynamic response of a typical BEDT-TTF salt.

| | |
|---|---|
| Resistivity anisotropy—$\rho_x:\rho_y:\rho_z$ (Ref. 1) | $\approx 1:1:10^3$ |
| In-plane conductivity—$\sigma_\parallel$ (Ref. 43) | $\approx 10^6\ \Omega^{-1}\ \mathrm{cm}^{-1}$ |
| In-plane skin depth—$\delta_\parallel$ (current $\parallel$ plane) | $\approx 1\ \mu$m |
| Interplane skin depth—$\delta_z$ (current $\perp$ plane) | $\approx 50\ \mu$m |
| Cyclotron radius at 1 T $-r_c$ | $\approx 1\ \mu$m |
| Mean-free path $\lambda = v_f \tau$ (assuming $\tau = 4\times 10^{-11}$ s) | $\approx 5\ \mu$m |
| Typical sample size | $1\times 1\times 0.2\ \mathrm{mm}^3$ |

this growth process, and then to control the growth rate in order to achieve a greater degree of uniformity.[42]

Finally, we note that the scattering times deduced from published CR data show a considerable sample dependence, as can be seen by comparing line widths obtained by different groups, for the $\alpha$-$(\mathrm{BEDT\text{-}TTF})_2\mathrm{NH}_4\mathrm{Hg}(\mathrm{NCS})_4$ salt.[20–22,24–26] These differences again reflect a distribution of sample quality.

## IV. EXPERIMENT

### A. The relevance of $\sigma_{zz}(\omega)$ to real experiments

In this section, we consider the experimental implications of our model for $\sigma_{zz}(\omega)$. As a starting point, Table I lists some of the key parameters that govern the electrodynamic response of a typical BEDT-TTF salt. We again choose $\alpha$-$(\mathrm{BEDT\text{-}TTF})_2\mathrm{NH}_4\mathrm{Hg}(\mathrm{NCS})_4$ as an example, and the parameters in Table I are based on 4.2-K data.

We can immediately rule out the likelihood of observing Azbel'-Kaner CR[33] and, therefore, Gor'kov-Lebed' CR,[30] from inspection of the above numbers. Observation of either of these effects requires that the cyclotron radius and mean-free path be considerably longer than the skin depth. In fact, the condition $(r_c/\delta) \gg (\omega\tau)^{1/2}$ should strictly be satisfied in order to observe these effects, where $r_c$ is the cyclotron radius and $\delta$ the skin depth.[44,45]

Next, we consider the following two situations: (i) an experiment where only in-plane ac currents are excited, and (ii) an experiment where only interplane ac currents are excited. In either case, we shall assume that we are in the relaxation limit, i.e., $\omega\tau \gg 1$, and that the magnetic field is applied normal to the conducting planes. The exact details of how we perform these experiments will be given below.

*Case (i).* Under these conditions, $\delta_\parallel \leqslant \lambda$, and we are on the verge of being in the anomalous skin effect regime, where the mean-free path ($\lambda$) should be much greater than the in-plane skin depth ($\delta_\parallel$).[44] In this regime, the relationship between the current density and the local electromagnetic field is not straightforward, thus ''classical'' electrodynamic theories no longer hold; here, we use the term ''classical'' to contrast the anomalous skin effect regime. Consequently, the penetration depth must be redefined according to

$$\delta^3 = \delta_0^2 \left( \frac{\lambda}{a} \right), \tag{9}$$

where $\delta_0$ is the ''classical'' skin depth and $a$ is a constant of order unity.[28,44] Equation (9) is not strictly valid in this particular case due to the fact that $\delta_\parallel$ is not ''much greater'' than $\lambda$. However, the net outcome will be that the condition $(r_c/\delta) \gg (\omega\tau)^{1/2}$ becomes even harder to satisfy. Therefore, it is highly unlikely that CR of the kind normally seen in metals, be observed under these conditions.

*Case (ii).* Under these conditions, $\delta_z > \lambda$, and we can adopt a simple ''classical'' approach to the problem.[28] Furthermore, because of the large interplane skin depth ($\delta_z$), which is comparable to the smallest sample dimension, we can assume that the bulk of the carriers in the sample contribute to the electrodynamic response. In this case, the energy absorbed from the electromagnetic radiation will simply be proportional to the dissipation in the sample, which is, in turn, proportional to $\rho_{zz}$ $[=1/\sigma_{zz}(\omega)]$. Hence, we see the importance here of $\sigma_{zz}(\omega)$.

We should reexamine case (i) at this point, since we cannot completely rule out dissipation effects similar to those considered for case (ii) above, i.e., we are not sufficiently far into the anomalous regime where we can ignore ''classical'' electrodynamic effects. The electrodynamic response under these conditions has been treated elsewhere,[27] in terms of the surface impedance of the sample. Therefore, it should be possible to observe conventional CR under these conditions. However, the predicted CR line shape is highly unusual in this case, as observed, e.g., recently in the organic conductor $(\mathrm{DMe\text{-}DCNQI})_2\mathrm{Cu}$,[27] and in semimetallic systems such as bismuth.[46] The symmetric Lorentzian resonances reported for BEDT-TTF salts[20–26] are reminiscent of the type of CR behavior observed for semiconducting systems. This fact, alone, suggests that the resonances observed in the Q2D salts must be due largely to the $z$-axis response, since the conductivity is so much lower in this direction, i.e., these are PORs and not CR.

Finally, we ask the question as to how it is that so many experiments pick up the $z$-axis response and yet they seem to be insensitive to the in-plane conductivity. The reason turns out to be relatively straightforward. All of the reported experiments are set up so that the ac electric and magnetic radiation fields act in a plane parallel to the conducting BEDT-TTF layers. Due to the experimental constraints associated with performing experiments at low temperatures and high fields, standing waves become a problem. In order to control these standing waves, resonant cavities have been used by some groups.[21,22,24,26–28] In this way, one can chose to place the sample either (I) at an electric (magnetic) field antinode (node) or (II) at a magnetic (electric) field antinode (node).[28] Case (I) corresponds to case (i) above, since the ac electric field will drive currents within the highly conducting BEDT-TTF layers. Case (II) causes currents to circulate in a plane perpendicular to the Q2D conducting layers; however, since the resistivity is highly anisotropic, dissipation will predominantly be due to inter-plane currents,[28] hence, case (II) corresponds to case (ii) above. As noted in Sec. II, no SdH oscillations are observed in case (I), suggesting that it is extremely hard to measure the conductivity in this direction. Furthermore, when care is taken to position the sample at a magnetic field antinode, very clear POR features are invariably observed. For measurements where cavities are not used,[19,20,23,25] control over the electromagnetic environment in the vicinity of the sample is impossible, and observation of PORs is, therefore, fortuitous.

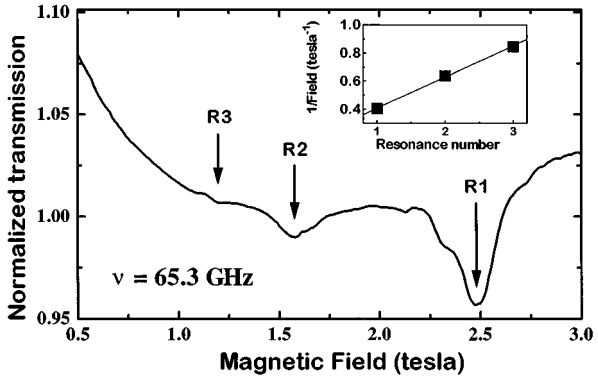


FIG. 5. Normalized transmission through a mosaic of $\alpha$-(BEDT-TTF)$_2$NH$_4$Hg(NCS)$_4$ crystals, from Ref. 22, the temperature is 1.2 K. Three resonances can be seen, labeled R1 to R3. The inset displays the resonance positions plotted against inverse field.

We have shown, in this section, how $\sigma_{zz}(\omega)$ can dominate the electrodynamic response of a Q2D conductor. Clearly, it would be nice to be able to probe the pure in-plane conductivity by this technique and, therefore, to observe conventional CR. In principle, this should be possible, provided interplane currents can be entirely eliminated. Further refinements of experimental technique are required to check this, and are currently under development.

### B. Discussion of existing magneto-optical data

As a conclusion to this experimental section, we show some real experimental data from Ref. 22. Figure 5 shows the transmission through a mosaic comprising about ten $\alpha$-(BEDT-TTF)$_2$NH$_4$Hg(NCS)$_4$ single crystals. Three resonances can be seen in Fig. 5, labeled R1 to R3; these resonances appear as sharp dips in the transmission. A reduction in the transmission through the sample mosaic corresponds to an increase in the reflectivity of the mosaic and, therefore, an increase in the conductivity of the samples in the mosaic; hence, we can confidently ascribe these features to cyclotron-like behavior, e.g., PORs.

The three resonances in Fig. 5 cannot be explained in terms of a simple CR picture. Therefore, we assume that these resonances are either Q1D or Q2D PORs. Unfortunately, no detailed studies of the angle dependence of these features have been reported, so it is not possible to determine the precise origin of each of the resonances. In one report, however, it is speculated that Q2D carriers are responsible for R1, and that Q1D carriers are responsible for R2;[26] R3 is not observed in this study.

The inset to Fig. 5 displays the resonance positions plotted against inverse field. It is apparent that these points lie on a straight line and are, therefore, periodic in 1/B; the periodicity is 0.222 T$^{-1}$, which corresponds to an effective mass of $1.9m_e$. The periodicity in 1/B suggests that the resonances originate from the same POR sequence (either Q2D or Q1D). However, the field positions are in the ratio $(\frac{1}{2}:\frac{1}{3}:\frac{1}{4})$, implying that the fundamental resonance is absent; this is not inconsistent with the simulations in Sec. III. Clearly, further experimental studies are necessary to clarify the origin of each resonance in Fig. 5.

## V. SUMMARY AND CONCLUSIONS

In this paper, we have discussed several aspects of the magneto-electrodynamic response of Q2D BEDT-TTF salts, both from a theoretical perspective, and from an experimental point of view. In particular, PORs are predicted for both Q2D and Q1D Fermi surfaces. These PORs will be observed as sequences of harmonics, periodic in 1/B, where the periodicity is related to the effective masses of either the Q2D or Q1D carriers. We go on to demonstrate how the conductivity in the least dispersive direction can dominate the electrodynamic response of highly anisotropic conductors. We have discussed compelling experimental evidence supporting our model, e.g., the observation of several CR for the simple metal $\alpha$-(BEDT-TTF)$_2$NH$_4$Hg(NCS)$_4$, and the success of measurements designed to probe the interplane response of the same material. In view of this, we urge caution when interpreting magneto-optical data, since our models for $\sigma_{zz}(\omega)$ indicate a nontrivial POR behavior in this direction, being highly sensitive to the precise shape of the Fermi surfaces—both Q2D and Q1D.

We also discuss other aspects arising from a semiclassical treatment of CR/POR, in particular, effects that lead to a broadening of resonances. Differences between the scattering times deduced from magneto-optical and SdH and/or dHvA measurements, suggest that sample inhomogeneities play an important role in the fermiology of organic conductors. Additionally, we have demonstrated that a $(d_{xx}+d_{yy})$ warping symmetry leads to dc magnetoresistance for current parallel to field, irrespective of whether the warping axis is tilted away from the cylinder axis.

The outcome of this work is a clearer picture of CR/POR in the BEDT-TTF salts. We avoid drawing too many conclusions from existing experimental data and, instead, point the way to future experiments. These experiments should be performed on small single crystals in a well controlled electromagnetic environment. It is also desirable to have a means to rotate the sample *in situ*, with respect to the applied dc magnetic field, whilst maintaining the same controlled electromagnetic environment. Of particular interest will be the temperature dependence of the resonance line shapes, which may hold important information about quasiparticle scattering mechanisms. It will also be important to differentiate between Q2D and Q1D contributions to the electrodynamic response, thereby, enabling an unambiguous determination of effective masses. Due to the similarity between PORs and AMRO, it should be possible to distinguish between the Q2D and Q1D POR contributions from their angle dependence. From the relative strengths of the POR subharmonics, one could, in principle, obtain information about the precise deformations of the Q2D and Q1D Fermi surfaces. This offers an exciting method for determining the fermiology of low-dimensional conductors.

## ACKNOWLEDGMENTS

This work was supported by the National Science Foundation under Grant No. NSF-DMR 95-10427. The authors would also like to thank Professor J. S. Brooks, Dr. S. Uji, and P. S. Sandhu for useful discussion.

[1] J. M. Williams, J. R. Ferraro, R. J. Thorn, K. D. Carlson, U. Geiser, H. H. Wang, A. M. Kini, and M. H. Whangbo, *Organic Superconductors (Including Fullerenes)-Synthesis, Structure, Properties, and Theory* (Prentice Hall, Englewood Cliffs, NJ, 1992).

[2] T. Ishiguro and K. Yamaji, *Organic Superconductors*, Springer Series in Solid State Sciences Vol. 88 (Springer-Verlag, Berlin, 1990).

[3] J. Wosnitza, *Fermi Surfaces of Low Dimensional Organic Metals and Superconductors*, Springer Tracts in Modern Physics Vol. 134 (Springer-Verlag, Berlin, 1996).

[4] For a review, see, e.g., Synth. Met. **69-71** (1995).

[5] D. Shoenberg, *Magnetic Oscillations in Metals* (Cambridge University Press, Cambridge, 1984).

[6] M. V. Kartsovnik, P. A. Kononovich, V. N. Laukhin, and I. F. Schegolev, Pis'ma Zh. Eksp. Teor. Fiz. **48**, 498 (1988) [JETP Lett. **48**, 541 (1988)].

[7] K. Yamaji, J. Phys. Soc. Jpn. **58**, 1520 (1989).

[8] T. Osada, A. Kawasumi, R. Yagi, S. Kagoshima, N. Miura, M. Oshima, H. Mori, T. Nakamura, and G. Saito, Solid State Commun. **75**, 901 (1990).

[9] R. Yagi, Y. Iye, T. Osada, and S. Kagoshima, J. Phys. Soc. Jpn. **59**, 3069 (1990).

[10] M. V. Kartsovnik, V. N. Laukhin, S. I. Pesotskii, I. F. Schegolev, and V. M. Yakovenko, J. Phys. (France) I **2**, 89 (1991).

[11] Y. Iye, R. Yagi, N. Hanasaki, S. Kagoshima, H. Mori, H. Fujimoto, and G. Saito, J. Phys. Soc. Jpn. **63**, 674 (1994).

[12] M. V. Kartsovnik, A. E. Kovalev, V. N. Laukhin, and S. I. Pesotskii, J. Phys. (France) I **2**, 223 (1993); M. V. Kartsovnik, A. E. Kovalev, and N. Kushch, *ibid.* **3**, 1187 (1993).

[13] T. Osada, S. Kagoshima, and N. Miura, Phys. Rev. B **46**, 1812 (1992).

[14] R. Yagi and Y. Iye, Solid State Commun. **89**, 275 (1994).

[15] S. J. Blundell and J. Singleton, Phys. Rev. B **53**, 5609 (1996).

[16] J. Caulfield, W. Lubczynski, F. L. Pratt, J. Singleton, D. Y. K. Ko, W. Hayes, M. Kurmoo, and P. Day, J. Phys. Condens. Matter **6**, 2911 (1994).

[17] N. Harrison, R. Bogaerts, P. Reinders, J. Singleton, S. J. Blundell, and F. Herlach, Phys. Rev. B **54**, 9977 (1996).

[18] P. S. Sandhu, G. J. Athas, J. S. Brooks, E. G. Haanappel, J. D. Goettee, D. W. Rickel, M. Tokumoto, N. Kinoshita, T. Kinoshita, and Y. Tanaka, Surf. Sci. **361/362**, 913 (1996).

[19] J. Singleton, F. L. Pratt, M. Doporto, W. Hayes, T. J. B. M. Janssen, J. A. A. J. Perenboom, M. Kurmoo, and P. Day, Phys. Rev. Lett. **68**, 2500 (1992).

[20] S. Hill, J. Singleton, F. L. Pratt, W. Hayes, T. J. B. M. Janssen, J. A. A. J. Perenboom, M. Kurmoo, and P. Day, Synth. Met. **55-57**, 2566 (1993).

[21] S. Hill, A. Wittlin, J. van Bentum, J. Singleton, W. Hayes, J. A. A. J. Perenboom, M. Kurmoo, and P. Day, Synth. Met. **70**, 821 (1995).

[22] S. Hill, Ph.D. thesis (University of Oxford, 1994).

[23] S. V. Demishev, A. V. Semeno, N. E. Sluchanko, N. A. Samarin, I. B. Voskoboinikov, V. V. Glushkov, J. Singleton, S. J. Blundell, S. O. Hill, W. Hayes, M. V. Kartsovnik, A. E. Kovalev, M. Kurmoo, P. Day, and N. D. Kushch, Phys. Rev. B **53**, 12 794 (1996).

[24] A. Polisskii, J. Singleton, P. Goy, W. Hayes, M. Kurmoo, and P. Day, J. Phys. C **8**, L195 (1996).

[25] H. Ohta, Y. Yamamoto, K. Akioki, M. Motokawa, and K. Kanoda, Synth. Met. (to be published); K. Akioki, H. Ohta, Y. Yamamoto, M. Motokawa, and K. Kanoda, *ibid*. (to be published); H. Ohta, Y. Yamamoto, K. Akioki, M. Motokawa, T. Sasaki, and T. Fukase, *ibid*. (to be published).

[26] A. Ardavan, J. Singleton, W. Hayes, A. Polisski, P. Goy, M. Kurmoo, and P. Day, Synth. Met. (to be published).

[27] S. Hill, P. S. Sandhu, M. Boonman, J. A. A. J. Perenboom, A. Wittlin, S. Uji, J. S. Brooks, R. Kato, H. Sawa, and S. Aonuma, Phys. Rev. B **54**, 13 536 (1996).

[28] O. Klein, S. Donovan, M. Dressel, and G. Grüner, Int. J. of Infrared Millim. Waves **14**, 2423 (1993); S. Donovan, O. Klein, M. Dressel, and G. Grüner, *ibid*. **14**, 2459 (1993); M. Dressel, O. Klein, S. Donovan, and G. Grüner, *ibid*. **14**, 2489 (1993).

[29] R. H. McKenzie, G. J. Athas, J. S. Brooks, R. G. Clark, A. S. Dzurak, R. Newbury, R. P. Starrett, A. Skougarevsky, M. Tokumoto, N. Kinoshita, T. Kinoshita, and Y. Tanaka, Phys. Rev. B **54**, 8289 (1996).

[30] L. P. Gor'kov and A. G. Lebed', Phys. Rev. Lett. **71**, 3874 (1993).

[31] We chose this compound as an example, since it remains metallic down to 1 K and, contrary to the other $\alpha$-phase salts, its Fermi surface is well known.

[32] C. E. Campos, P. S. Sandhu, J. S. Brooks, and T. Ziman, Phys. Rev. B **53**, 12 725 (1996).

[33] M. Ya. Azbel' and E. A. Kaner, Zh. Eksp. Teor. Fiz. **32**, 896 (1956) [Sov. Phys. JETP **5**, 730 (1957)].

[34] S. Hill, S. Uji, P. S. Sandhu, J. S. Brooks, and L. Seger, Synth. Met. (to be published).

[35] J. M. Ziman, *Principles of the Theory of Solids* (Cambridge University Press, Cambridge 1972).

[36] The conduction bands of metallic BEDT-TTF salts are primarily based on linear combinations of the highest occupied molecular orbitals (HOMOs) of the BEDT-TTF molecules. The HOMOs are $\pi$-orbitals, which extend perpendicular to the plane of the molecule and are, therefore, oriented nearly parallel to the plane of the BEDT-TTF layers. Only the C-H bonds of the BEDT-TTF molecules are pointed towards the anion layers. Therefore, the HOMO's of BEDT-TTF molecules residing in one layer cannot interact (i.e., overlap) with those of BEDT-TTF molecules residing in adjacent layers. This consideration suggests that the conduction band, being made up of the HOMOs of BEDT-TTF molecules, cannot be dispersive along the interlayer direction. Thus, if there is any nonzero dispersion along the interlayer direction, experimentally or theoretically (based on accurate calculations), it is not due to HOMO-HOMO overlap integrals, but to something else. At present, it is not known what this ''something'' is; M. H. Whangbo (private communication).

[37] Momentum is, of course, still conserved in this direction. The changing $z$-axis velocity merely reflects the $k_x, k_y$ dependence of $m_{zz}$, the $z$ component of the effective mass tensor.

[38] We note, that for larger angles, particularly at angles greater than the positions of the first AMRO peaks, the POR behavior will become a lot more complex; the $z$-axis velocity will undergo many cycles during a single cyclotron period. Further work on the angle dependence of PORs is in preparation.

[39] Although it is difficult to be absolutely sure of the current path in a measurement of $\rho_{zz}$, it is expected that dissipation due to

interplane currents will overwhelm the contribution from in-plane currents, due to the highly anisotropic resistivity tensor ($\rho_x:\rho_y:\rho_z \approx 1:1:10^3$).

[40] The $z$-axis bandwidth [$\propto \sqrt{(\delta_x^2+\delta_y^2)}$] appears in the constant prefactor in Eq. (6), and therefore controls the strength of the PORs.

[41] Inhomogeneities on a macroscopic scale may result from varying strains in the sample.

[42] N. Fortune and Y. Kobayashi, Synth. Met. (to be published).

[43] M. Dressel, J. E. Eldridge, H. H. Wang, U. Geiser, and J. M. Williams, Synth. Met. **55-57**, 2923 (1993).

[44] A. A. Abrikosov, *Fundamentals of the Theory of Metals* (Elsevier, Amsterdam, 1988).

[45] In the case of Q1D CR, $r_c$ is replaced by a parameter which represents the amplitude of the sinusoidal real space trajectories of the Q1D carriers; see Ref. 30.

[46] J. K. Galt, W. A. Yager, F. R. Merritt, B. B. Cetlin, and A. D. Brailsford, Phys. Rev. **114**, 1396 (1959); J. K. Galt, W. A. Yager, F. R. Merritt, B. B. Cetlin, and H. W. Dail, *ibid.* **100**, 748 (1955).